Distribution of dissolved organic nutrients and their effect on export production over the Atlantic Ocean

S. Torres-Valdés,[1] V. M. Roussenov,[2] R. Sanders,[1] S. Reynolds,[2,3] X. Pan,[1,3] R. Mather,[2] A. Landolfi,[1,4] G. A. Wolff,[2] E. P. Achterberg,[1] and R. G. Williams[2]

Received 26 September 2008; revised 29 May 2009; accepted 28 July 2009; published 3 November 2009.

[1] A synthesis is provided of dissolved organic nitrogen (DON) and phosphorus (DOP) distributions over the Atlantic Ocean based upon field data from eight recent transects, six meridional between 50°N and 50°S and two zonal at 24° and 36°N. Over the entire tropical and subtropical Atlantic, DON and DOP provide the dominant contributions to total nitrogen and phosphorus pools for surface waters above the thermocline. Elevated DON and DOP concentrations (>5 and >0.2 μmol L^{-1}, respectively) occur in surface waters on the eastern side of the North Atlantic subtropical gyre and equatorial sides of both the North and South Atlantic subtropical gyres, while particularly low concentrations of DOP (<0.05 μmol L^{-1}) occur over the northern flank of the North Atlantic subtropical gyre along 36°N. This distribution is consistent with organic nutrients formed at the gyre margins supporting carbon export as they are redistributed via the gyre circulation. The effect of DON and DOP transport and cycling on export production is examined in an eddy-permitting, coupled physical and nutrient model integrated for 40 years: organic nutrients are produced in the upwelling zones off North Africa and transferred laterally into the gyre interior, facilitated in part by the mesoscale eddy circulation, as well as fluxed northward from the tropics as part of the overturning circulation. Inputs of semilabile DON and DOP to the tropical and subtropical Atlantic Ocean play an important role in sustaining up to typically 40 and 70% of the modeled particulate N and P export, particularly on the eastern and equatorward sides of the subtropical gyres.

Citation: Torres-Valdés, S., V. M. Roussenov, R. Sanders, S. Reynolds, X. Pan, R. Mather, A. Landolfi, G. A. Wolff, E. P. Achterberg, and R. G. Williams (2009), Distribution of dissolved organic nutrients and their effect on export production over the Atlantic Ocean, *Global Biogeochem. Cycles*, *23*, GB4019, doi:10.1029/2008GB003389.

1. Introduction

[2] Export production over the extensive oligotrophic subtropical gyres is thought to account for up to half of global oceanic carbon export [*Emerson et al.*, 1997, 2001]. In the Sargasso Sea, export production has been estimated to be in excess of 4 mol C m^{-2} yr^{-1} [*Jenkins*, 1982; *Jenkins and Goldman*, 1985], requiring a nutrient supply of at least 0.6 mol N m^{-2} yr^{-1} and ~38 mmol P m^{-2} yr^{-1} if Redfield stoichiometry is assumed. A range of mechanisms have been invoked for the provision of nutrients to the euphotic zone, including atmospheric deposition, convection, diapycnal diffusion and N_2 fixation; however, rates of nutrient supply by these processes are thought to fall short of the levels required to sustain the inferred export production (see reviews by *McGillicuddy et al.* [1998], *Williams and Follows* [2003], and *Pelegrí et al.* [2006]). The process of N_2 fixation would require an additional source of phosphorous [*Mahaffey et al.*, 2004], whilst atmospheric deposition provides nutrient inputs with N to P ratios far above Redfield stoichiometry [*Baker et al.*, 2003].

[3] A possible mechanism to sustain export production in oligotrophic gyres is the supply of dissolved organic matter (DOM) to the euphotic zone. For this mechanism to be important, DOM needs to be transferred from productive upwelling zones into the interior of the oligotrophic gyres within the upper ocean. The surface geostrophic circulation can easily redistribute tracers over much of the subtropical gyres through narrow western boundary currents, gyre-scale flows, and mesoscale eddies [*Pelegrí and Csanady*, 1991; *Williams and Follows*, 2003; *Williams et al.*, 2006]. Along gyre boundaries, the wind-driven Ekman transfer also becomes important in transferring inorganic nutrients [*Williams and Follows*, 1998] and DOM [*Mahaffey et al.*, 2004] into the subtropical gyres.

[4] In support of this view, DOM concentrations have been found to dominate the nitrogen and phosphorus pools

[1]National Oceanography Centre, University of Southampton, Southampton, UK.
[2]Department of Earth and Ocean Sciences, University of Liverpool, Liverpool, UK.
[3]Now at British Oceanographic Data Centre, Liverpool, UK.
[4]Now at Marine Biogeochemie, Leibniz-Institut Für Meereswissenschaften, Kiel, Germany.

0886-6236/09/2008GB003389

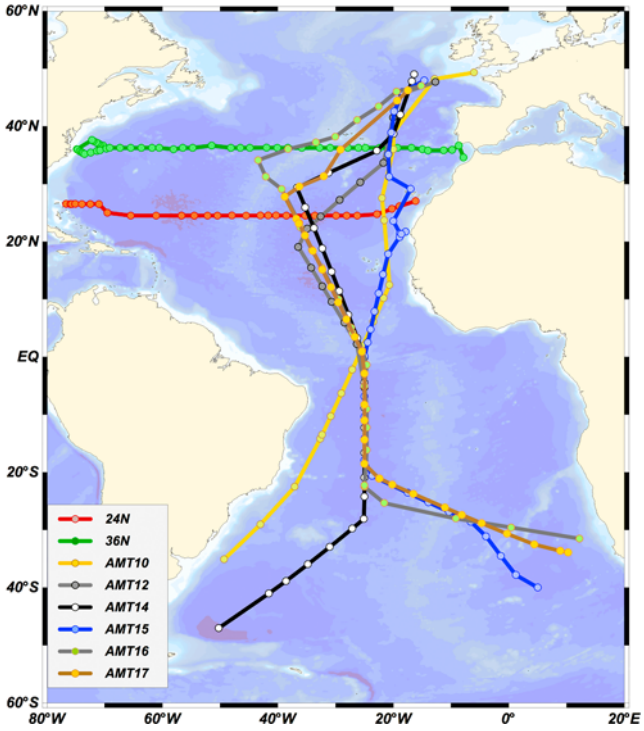

Figure 1. Map showing cruise tracks and position of stations where samples for organic nutrient analysis were collected during cruises AMT10, AMT12, AMT14, AMT15, AMT16, AMT17, 24°N, and 36°N. Produced using Ocean Data View (R. Schlitzer, Ocean data view, 2009, available at http://odv.awi.de).

in the euphotic zone over the oligotrophic gyres [e.g., *Vidal et al.*, 1999; *Abell et al.*, 2000; *Mahaffey et al.*, 2004]. The presence of DOM is only important though if the DOM can ultimately enhance the nutrient supply to primary producers: labile forms of the dissolved organic nitrogen (DON) pool can be taken up by primary producers [*Antia et al.*, 1991; *Bronk*, 2002; *Berman and Bronk*, 2003; *Bronk et al.*, 2007], while semilabile forms may be broken down by bacterial activity and by phytoplankton proteolytic enzymes (intracellular or extracellular) and thus become available [*Bronk et al.*, 2007]. Part of the refractory DON pool can also become bioavailable upon exposure to natural UV photo-oxidation processes [*Bushaw et al.*, 1996] and/or bacterial degradation [*Bronk et al.*, 2007]. The dissolved organic phosphorus (DOP) pool is mostly bioavailable [*Karl and Yanagi*, 1997; *Björkman et al.*, 2000; *Karl and Björkman*, 2002] and preferentially remineralized (mainly by bacterial transformations) from DOM relative to nitrogen and carbon [*Clark et al.*, 1998; *Kolowith et al.*, 2001]. However, despite the potential importance of DON and DOP, there has not been a systematic mapping of their basin-scale distributions, apart from a few large-scale surveys [e.g., *Vidal et al.*, 1999; *Moutin et al.*, 2008].

[5] In support of this mechanism, a recent modeling study by *Roussenov et al.* [2006] suggested that the horizontal transport of DON and DOP can provide nutrient inputs to sustain a significant fraction of export production over the North Atlantic subtropical gyre. The controlling mechanism involves an interplay of DOM production, transport and utilization: DOM is preferentially formed in upwelling zones along the equatorial region and off the northwest African coast. The semilabile and refractory fractions of DOM, with lifetimes of months to years, are transported away from these formation regions. DOM is horizontally transported within the mixed layer, then partly utilized in summer, sustaining extra phytoplankton growth, which in turn produces a smaller concentration of DOM that is again transported into the gyre interior [*Williams and Follows*, 1998; *Roussenov et al.*, 2006].

[6] In the present work we focus on the North Atlantic subtropical gyre and assess the hypothesis that DON and DOP provide an important nutrient supply, therefore contributing to export production. Firstly, the large-scale distributions of DON and DOP are mapped over the tropical and subtropical Atlantic Ocean in order to test whether their patterns are consistent with this hypothesis. For this, data from six recent Atlantic Meridional Transects (AMT) and two zonal transects (24°N and 36°N), are presented. Second, the potential effect of the transport and cycling of DON and DOP on export production is assessed using an eddy-permitting model of the Atlantic Ocean, integrated for 40 years with a resolution of 0.23° × 0.23°, extending the previous coarser-resolution study of *Roussenov et al.* [2006].

2. Methods

[7] The observational approach is now set out, including the distribution of cruises and the analysis techniques employed for the dissolved organic nutrients.

2.1. Oceanographic Surveys

[8] In order to reveal the dissolved organic nutrient distributions, six meridional cruises were conducted in the Atlantic Ocean and two zonal cruises in the North Atlantic between spring 2000 and autumn 2005 (Figure 1 and Table 1). The effort described here makes use of cruises within the AMT framework (http://www.amt-uk.org), a programme designed to evaluate basin-scale biogeochemistry in the entire Atlantic and hydrographic cruises which undertake full depth CTD sections across the North Atlantic to measure heat transport. The AMT cruises were designed to sample different gyre and upwelling regimes in the Atlantic between 50°N and 50°S: the transects crossed the eastern side of the North Atlantic subtropical gyre, extending from 45°W in the gyre interior to 18°W close to the coastal upwelling, usually passing along 25°W from the equator to around 30°S through the South Atlantic subtropical gyre, and then extending through the southwestern and southeastern parts of the South Atlantic (Figure 1). The two zonal cruises crossed the North Atlantic from coast to coast along 24.5°N and 36°N in order to close property budgets: the 24°N transect passes through the southern side of the North Atlantic subtropical gyre, while the 36°N transect passes through its northern flank, including where the Gulf Stream separates from the coast.

Table 1. Cruise Information[a]

Cruise	Research Ship	Cruise Track	Dates	Stns	Report
AMT 10	RRS *James Clark Ross*	33.08°S to 49.32°N	12 April to 8 May 2000	18	*Gallienne* [2000]
AMT 12	RRS *James Clark Ross*	50.09°S to 49.25°N	12 May to 17 June 2003	15	*Jickells* [2003]
AMT 14	RRS *James Clark Ross*	48.25°S to 49.25°N	28 April to 1 June 2004	28	*Holligan* [2004]
AMT 15	RRS *Discovery*	48.75°N to 40.00°S	17 September to 29 October 2004	32	*Rees* [2004]
AMT 16	RRS *Discovery*	31.52°S to 47.00°N	20 May to 29 June 2005	30	*Bale* [2005]
AMT 17	RRS *Discovery*	46.23°N to 33.91°S	15 October to 28 November 2004	32	*Holligan* [2005]
24°N	RRS *Discovery*	−79.93°W to −13.37°W	April to May 2004	25	*Cunningham* [2005]
36°N	RRS *Charles Darwin*	−74.81°W to −7.82°W	1 May to 15 June 2005	48	*McDonagh* [2007]

[a]Stns, number of stations where samples for organic nutrient measurements were taken. The meridional cruises are part of the Atlantic Meridional Transect (AMT) Programme [*Robinson et al.*, 2006a, 2006b] (see http://www.amt-uk.org). The zonal cruise at 36°N is part of the consortium programme of same name (http://www.bodc.ac.uk/36n), and the 24°N zonal cruise was part of the core strategic research programme "Ocean Variability and Climate" at the National Oceanography Centre, Southampton, United Kingdom [*Bryden et al.*, 2005; *Cunningham*, 2005]. Data are available at the British Oceanographic Data Centre (BODC) (http://www.bodc.ac.uk.)

2.2. Sample Collection and Analysis

2.2.1. Dissolved Inorganic Nutrients

[9] Samples for the analysis of dissolved inorganic nutrients, NO_3^- + NO_2^- (hereafter NO_3^-) and PO_4^{3-} were collected directly into 30 mL sterile polystyrene diluvials and analyzed onboard immediately after collection using colorimetric techniques. Analyses were carried out using either a Bran + Luebbe (AMT cruises) or a Skalar San^{plus} (24°N and 36°N) segmented flow autoanalyzer. Limits of detection were 0.03 μmol L^{-1} for both NO_3^- and PO_4^{3-} using the Bran + Luebbe autoanalyzer [*Holligan*, 2004; *Rees*, 2004] and 0.15 and 0.03 μmol L^{-1} for NO_3^- and PO_4^{3-}, respectively, using the Skalar autoanalyzer [*Cunningham*, 2005; *McDonagh*, 2007].

2.2.2. Total Dissolved Nutrients and Dissolved Organic Nutrients

[10] Seawater was collected in sterile 60 mL polystyrene vials and returned to shore frozen at −20°C for the determination of organic nutrients [*Sanders et al.*, 2005]. Only samples from the AMT10, 12, 14, 16, and 17 and 36°N cruises were filtered (47 mm Ø, 0.7 μm GF/F filters combusted at 450°C for 4 h). At each sampling station, 5 to 24 samples were collected down to ~5000 m, with a higher vertical resolution (5 to 12 samples) either in the upper 500 m of the water column or within the euphotic layer (down to 0.1% of surface irradiance). Further details can be found in Table 1 and citations therein.

[11] During the 36°N cruise, filtered and unfiltered seawater was collected in order to test whether differences in the organic nutrient determinations emerged due to the particle content within 60 mL of seawater. Analyses revealed no significant differences between filtered and unfiltered samples (Figures 2a and 2b), probably because the particulate pools (N and P) are small relative to the dissolved organic nutrient pools, suggesting that comparison between different cruises with or without filtering is valid. Henceforth, the terms total dissolved nitrogen (TDN) and total dissolved phosphorus (TDP) are used. Dissolved organic nitrogen (DON) and dissolved organic phosphorus (DOP), are further obtained as the difference between the total and the inorganic concentrations as described in section 2.2.4.

2.2.3. UV Versus HTC: Oxidation Efficiency

[12] An important caveat in the interpretation of DON data is related to the oxidation efficiency of the techniques employed. There are three methods commonly used for seawater analysis [*Bronk et al.*, 2000; *Sharp*, 2002]: ultraviolet photo-oxidation (UV), high-temperature combustion (HTC) and persulphate oxidation (PO).

[13] In this study, most TDN and TDP samples from all cruises were converted to PO_4^{3-} and NO_3^- after photo-oxidation for 2 h using a Metrohm 705 UV digester system [*Sanders and Jickells*, 2000]. These were subsequently analyzed using colorimetric techniques as described above. The UV method has the advantage of (1) allowing the simultaneous determination of nitrogen (N) and phosphorus (P), (2) producing comparatively low blanks for both N and P [*Sanders and Jickells*, 2000; *Landolfi*, 2005], (3) having a high oxidation efficiency for P and acceptable efficiency for N, and (4) involving less chemical manipulation as compared with the PO method. The UV oxidation efficiency is assessed throughout the analyses using various organic N and P containing compounds of different labilities (summarized in Table 2), which reveal oxidation efficiencies of up to 80% for N and 100% for P. Detection limits for TDN and TDP using the UV method were 0.45 μmol L^{-1} and 0.03 μmol L^{-1}, respectively. Given that the PO and HTC methods are known to achieve higher oxidation efficiencies for N [*Bronk et al.*, 2000], the PO method [*Valderrama*, 1981] was also assessed following *Bronk et al.* [2000], but it produced unacceptably high blanks even after recrystallizing the persulphate 2 or 3 times.

[14] In addition, sets of duplicate TDN samples were also processed using the HTC method for the 24°N and 36°N cruises using a Shimadzu 5000A DOC analyzer coupled to a Antek 705E chemiluminescent nitrogen detector [*Alvarez-Salgado and Miller*, 1998; *Landolfi*, 2005]. The HTC efficiency was 96–100% as tested with caffeine standard solutions [*Landolfi et al.*, 2008]. The accuracy of the method was tested by measuring consensus reference materials (CRM, available from Hansell Research Laboratory, University of Miami, Florida). It was within 5% of CRM concentrations for both zonal cruises. Limits of detection with this technique were 1.2 μmol L^{-1} for N. Data set comparisons show higher HTC-TDN concentrations for the

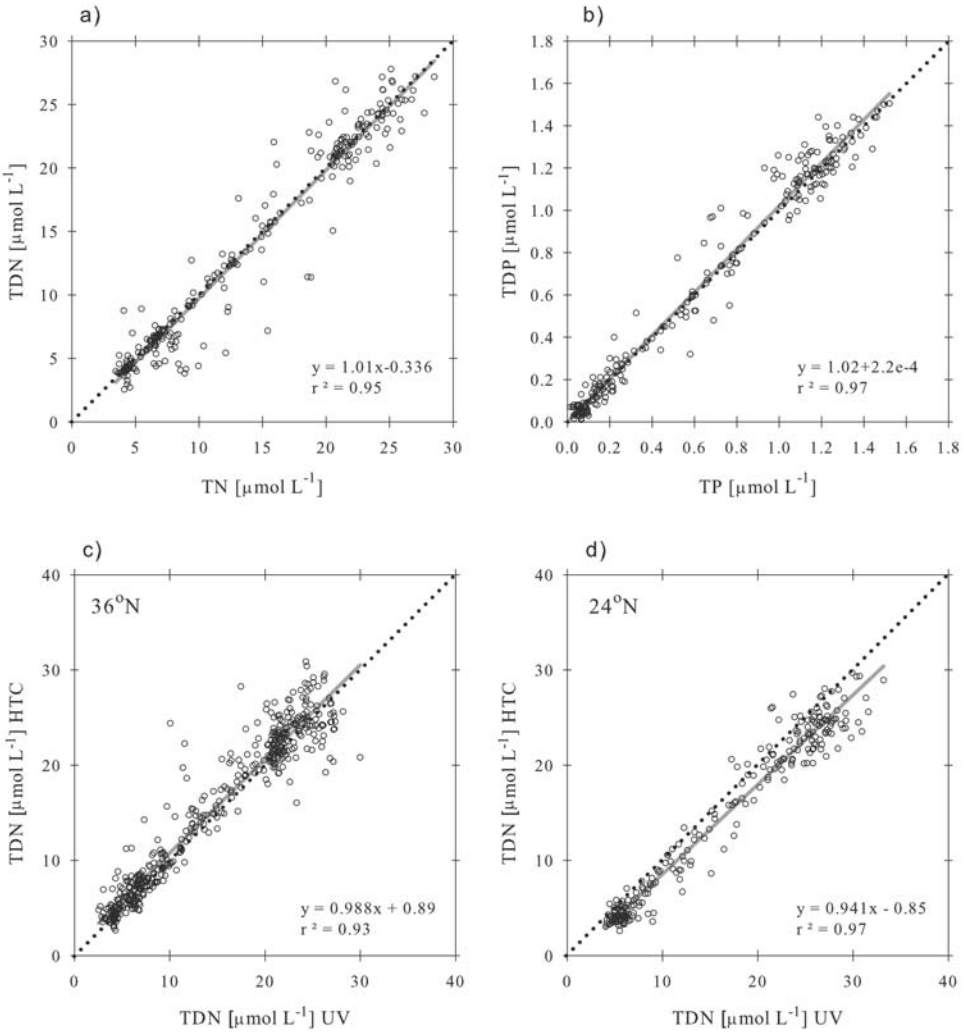

Figure 2. (top) (a) Total dissolved nitrogen (TDN) plotted against total nitrogen (TN) and (b) total dissolved phosphorus (TDP) plotted against total phosphorus (TP); i.e., filtered versus unfiltered samples (n = 265 for N, and n = 237 for P). (bottom) HTC-TDN plotted against UV-TDN; (c) 36°N (n = 502) and (d) 24°N (n = 251). Dotted lines are the 1:1 relation, and thick dark lines are the regression lines for the equations shown.

36°N samples (UV-[DON] within 4 ± 15% of HTC-[DON]), but slightly lower (within 14 ± 13% of UV-[TDN]) than the UV-TDN for the 24°N (Figures 2c and 2d).

2.2.4. DON and DOP

[15] DON and DOP were estimated by subtracting the inorganic from the total concentration, so that [DON] = [TDN] − [NO_3^-] and [DOP] = [TDP] − [PO_4^{3-}]. In the upper ocean where inorganic nutrients are present at nanomolar concentrations, detection limits for TDN and TDP represent the detection limits for DON and DOP as well. With the exception of AMT10 [*Mahaffey et al.*, 2004], organic nutrient analyses were carried out by the authors at the nutrient analysis facility of the National Oceanography Centre, Southampton, United Kingdom.

3. Field Observations

[16] The DON and DOP distributions are, firstly, reported in terms of their variation along meridional and zonal

Table 2. Nitrogen and Phosphorus Percent Recovery From Selected Organic Compounds After a 2 h UV Digestion[a]

Compound	Percent Nitrogen (n)	Percent Phosphorus (n)
(−)-Adenosine 5′-monophosphate (A5MP)	66 ± 13 (137)	102 ± 11 (135)
Guanosine 5′-monophosphate	42 ± 8 (115)	74 ± 12 (115)
2-Aminoethylphosphonic acid	84 ± 26 (43)	101 ± 11 (43)
Phytic acid sodium salt (PA)	-	67 ± 10 (72)
PA + A5MP	42 ± 13 (10)	76 ± 22 (10)
Caffeine	76 ± 8 (54)	-
Urea	79 ± 9 (22)	-
EDTA	48 ± 8 (34)	-
Urea + EDTA	2 ± 2 (19)	-

[a]Target concentration ranges were 2.5–10 μmol N L^{-1} and 1–2.5 μmol P L^{-1}. These solutions were prepared using a saline matrix (40 g NaCl L^{-1} of Milli-Q water), which was also used as analytical blank.

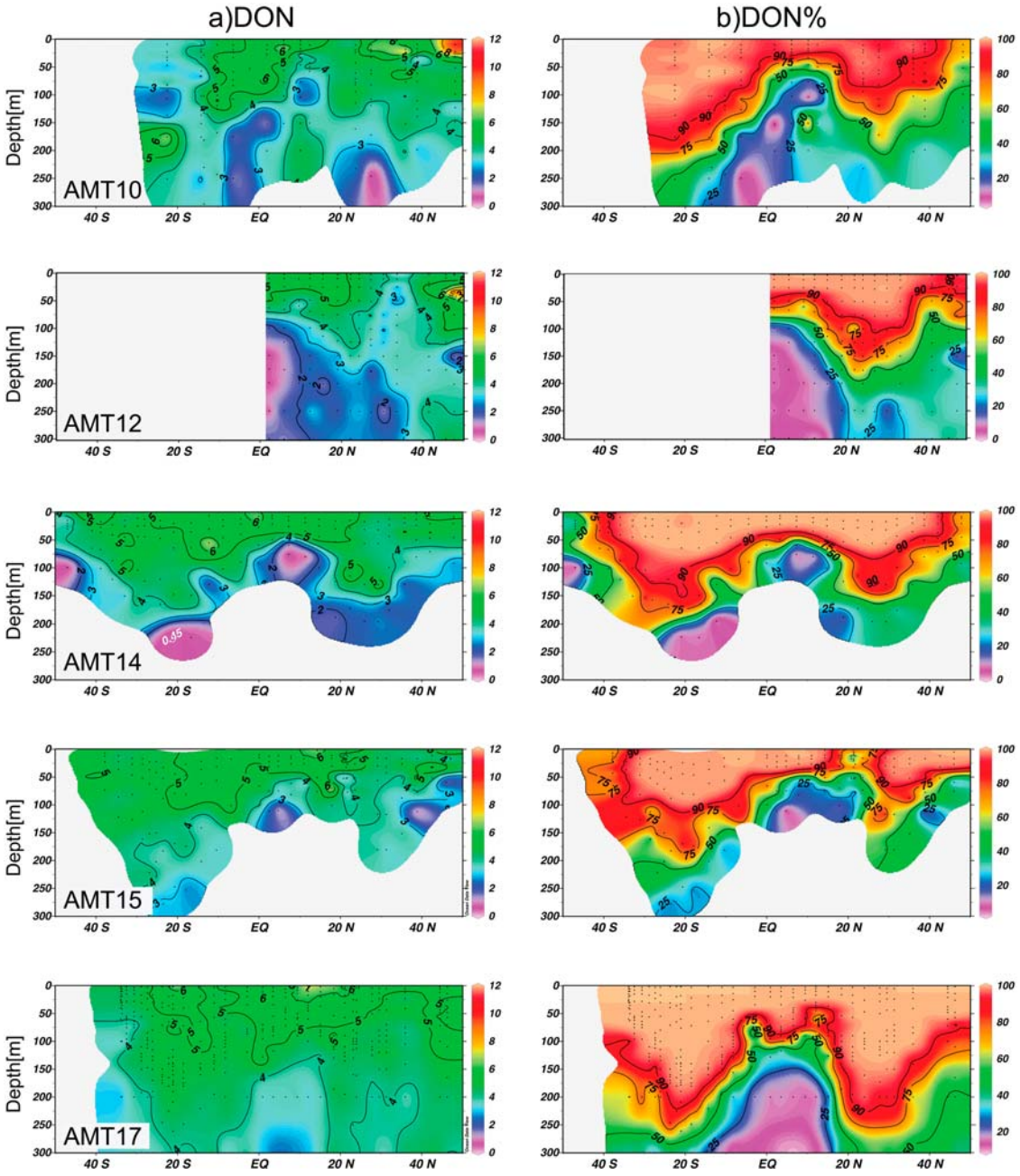

Figure 3. Meridional transects for (a) Dissolved organic nitrogen (DON; μmol L^{-1}) and (b) percentage of total nitrogen provided by DON from AMT10, AMT12, AMT14, AMT15, and AMT17. White represents regions with no data. All analyses use the UV photo-oxidation method, apart from AMT17 that uses the HTC method. Produced using Ocean Data View (Schlitzer, 2009).

transects and, secondly, in terms of composite maps based on the data gathered in the surface waters (upper 100 m).

3.1. DON and DOP Meridional and Zonal Sections

[17] DON and DOP concentrations are highest in the upper 300 m of the water column (Figures 3 and 4), reflecting the production of organic nutrients in the euphotic zone and their transport by the circulation. Over the meridional transects, DON concentrations range from maxima of typically 5 to 6 μmol L^{-1} to minima of less than 2 μmol L^{-1} (Figure 3a). The highest values occur within the upper 50 to 100 m, while lower values occur at greater depths. In comparing the individual transects, there is significant variability, highlighting how the dissolved organic nutrient distributions vary in time, reflecting seasonal and interannual variability (Table 1), as well as possible spatial differences (Figure 1). It is difficult to explain all of this detailed variability, but there are some consistent features. Higher DON concentrations are confined over the upper 50 m in the

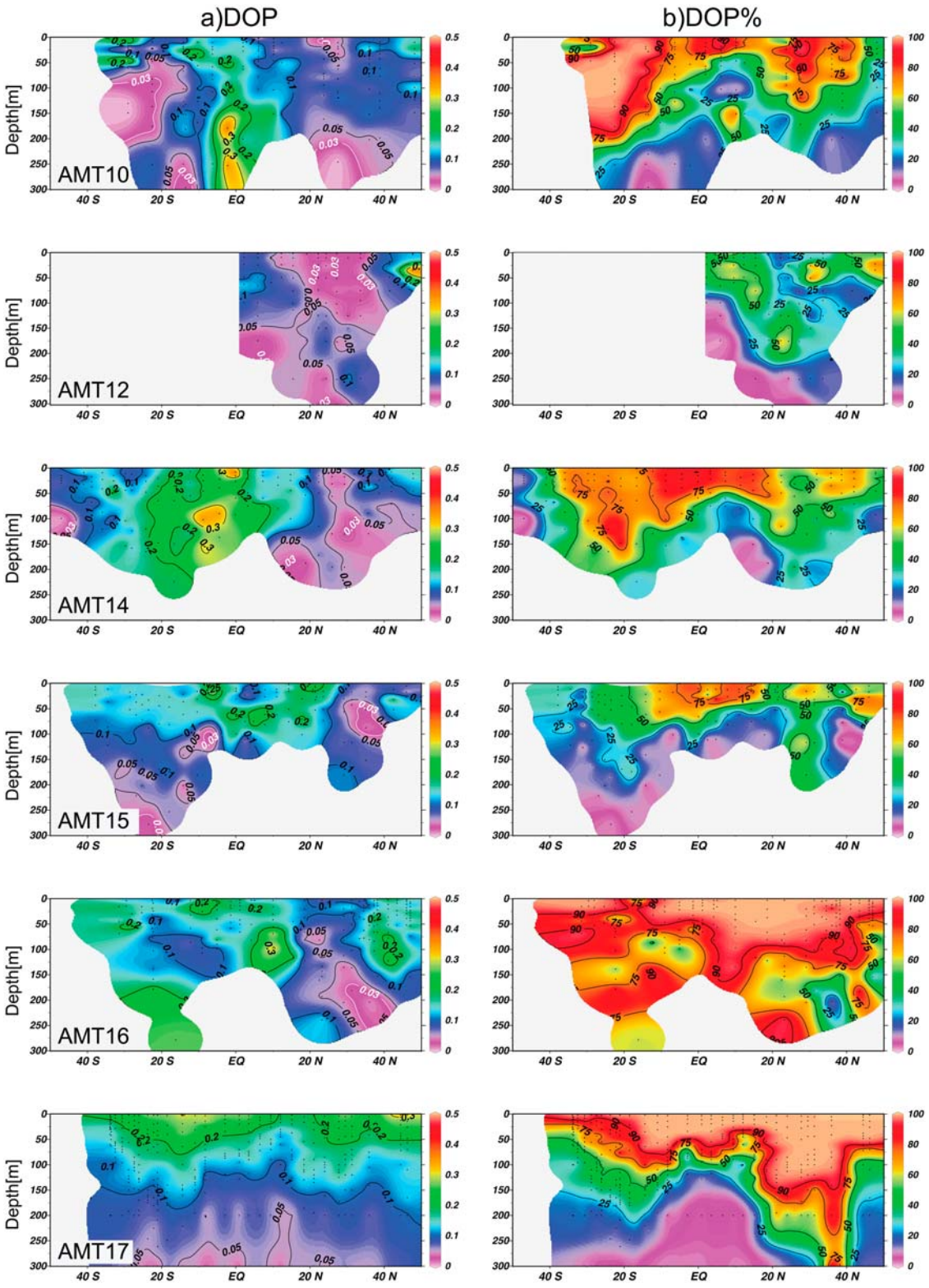

Figure 4. Meridional transects for (a) dissolved organic phosphorus (DOP; μmol L^{-1}) and (b) percentage of total phosphorus provided by DOP from AMT10, AMT12, AMT14, AMT15, AMT16, and AMT17. White isolines represent the DOP limit of detection (0.03 μmol L^{-1}). White represents regions with no data. All analyses use the UV photo-oxidation method. Produced using Ocean Data View (Schlitzer, 2009).

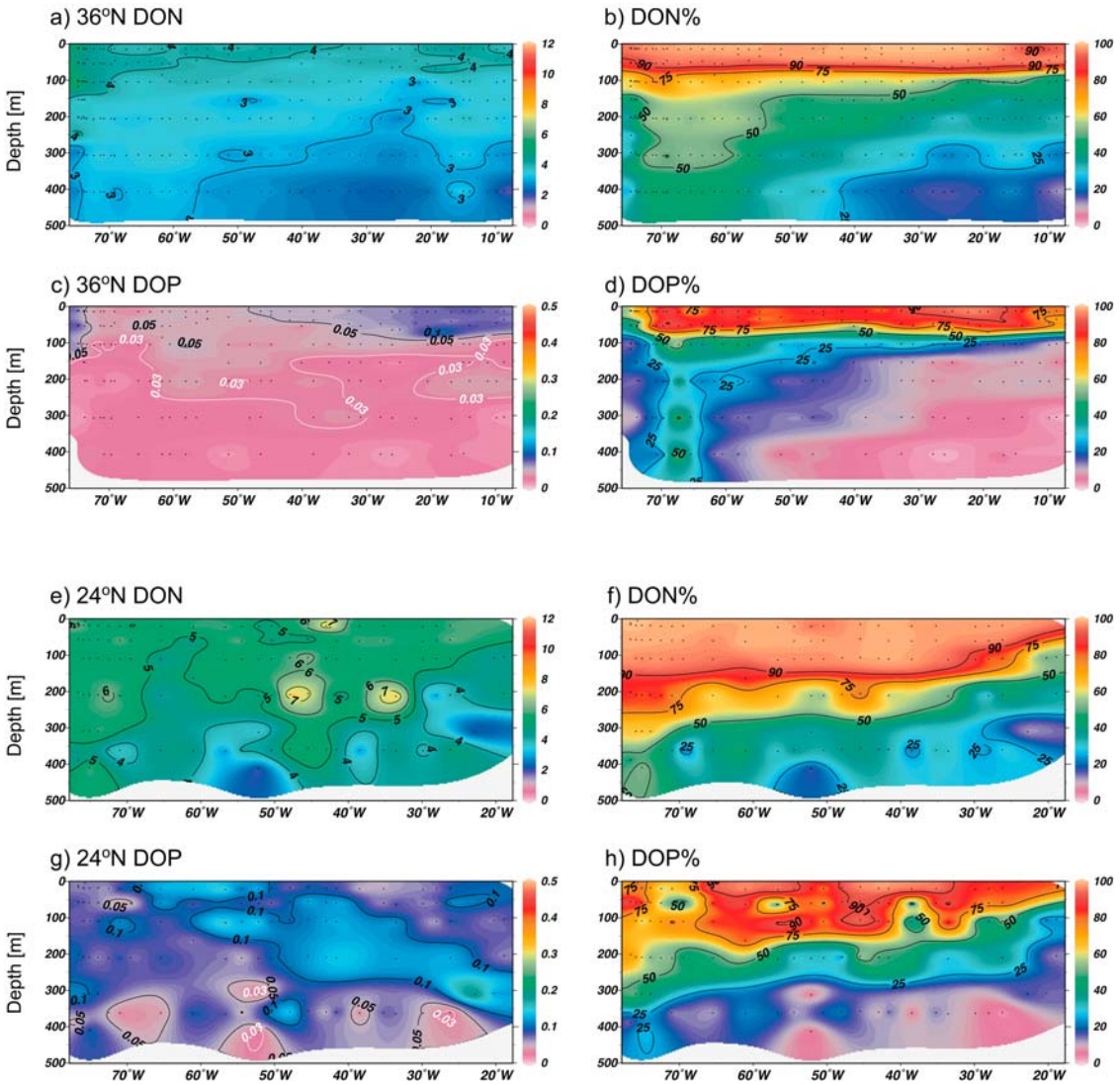

Figure 5. Zonal transects for (a, c, e, and g) dissolved organic nitrogen (DON; μmol L^{-1}) and dissolved organic phosphorus (DOP; μmol L^{-1}) along 36°N and 24.5°N together with (b, d, f, and h) percentage of total nitrogen provided by DON and percentage of total phosphorus provided by DOP. White isolines represent the DOP limit of detection (0.03 μmol L^{-1}). White represents regions with no data. All analyses use the UV photo-oxidation method. Produced using Ocean Data View (Schlitzer, 2009).

tropics, associated with the thermocline and nutricline being raised toward the sea surface, while higher values of DON extending to depths of 100 m or more are associated with the deepening of the thermocline over the subtropical gyres. There are generally slightly lower concentrations of DON over the North Atlantic (3–5 μmol L^{-1}) compared with the South Atlantic (4–5 μmol L^{-1}).

[18] DON dominates the total dissolved nitrogen (TDN) pool over these surface waters, accounting for more than 90% of the TDN (Figure 3b). The fractional contribution of the DON to total nitrogen again reflects the gyre-scale pattern of the thermocline: DON makes a dominant contribution for waters above the thermocline, but less important within the thermocline due to greater concentrations of nitrate.

[19] The DOP concentrations also vary over the basin (Figure 4a): within the upper 100 m, maxima occur in the tropics or parts of the South Atlantic subtropical gyre, reaching values of 0.2 to 0.3 μmol L^{-1}, while there are minima of 0.05 μmol L^{-1} or less over the North Atlantic subtropical gyre. There are year on year differences with the DOP minima in the North Atlantic subtropical gyre, being most apparent for the western transects AMT12, AMT14 and AMT16, still evident for the eastern transect AMT15, but absent for the western transect AMT17. Again DOP provides the dominant contribution to the total dissolved phosphorus (TDP), accounting for more than 75% of phosphorus in the upper 50 m along the transects (Figure 4b).

[20] The zonal transects across the North Atlantic subtropical gyre reveal less striking contrasts than seen in the

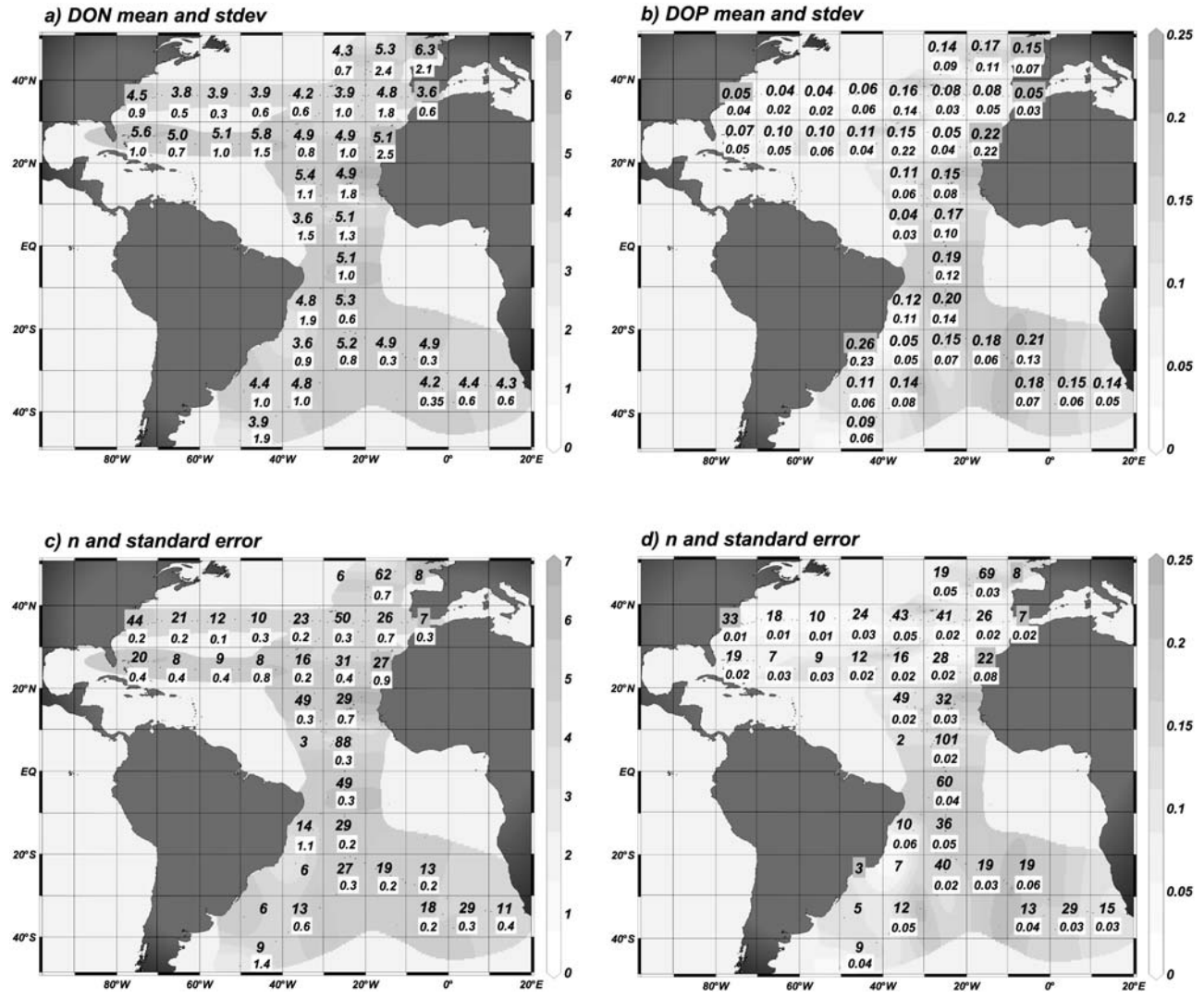

Figure 6. Statistics for DON and DOP sampling over the upper 100 m in the Atlantic: (a, b) mean and standard deviation (σ) in each 10° cell; (c, d) number of independent data points (n) given by the number of stations and the implied standard error ($\sigma/n^{1/2}$). Produced using Ocean Data View (Schlitzer, 2009).

meridional transects across the basin within the upper 100 m (Figure 5). DON appears to be relatively uniform along the west-east transects (varying <1 μmol L^{-1}), although there are higher concentrations along the 24.5°N transect (>4 μmol L^{-1}; Figure 5e) closer to the tropics than seen along the 36°N transect (3–4 μmol L^{-1}; Figure 5a). There is more variability in the DOP concentrations: slightly higher concentrations of DOP to the west along 24.5°N (Figure 5g), but conversely slightly higher DOP concentrations to the east along 36°N (Figure 5c). As seen before, the DON and DOP again provide the dominant contributions to TDN and TDP (Figures 5b, 5d, 5f, and 5h), respectively over the upper 100 m along 36°N and the upper 200 m along 24.5°N.

3.2. Composite Surface Maps for DON and DOP

[21] Given this data set for DON and DOP, we wish to construct composite maps for their surface variation over the Atlantic basin. However, the meridional sections reveal significant interannual variability in the data, so care needs to be taken when melding the data together.

[22] Consequently, we start by considering the data variability within 10° by 10° latitude-longitude cells over the basin. For each cell, all of the data over the upper 100 m is averaged together to form a mean and standard deviation (σ), where the standard deviation conveys how variable the data is. To gain confidence in how representative the mean is, the number of independent data points (n) are taken from the number of stations and a standard error is evaluated, $\sigma/n^{1/2}$; note that n is not taken from all the data points, as many samples from a single station need not be independent of each other, but samples from different stations (usually separated by 100 km or more) are viewed as being independent.

[23] Differences in the mean of DON and DOP for each cell over the basin typically reach 2 to 3 μmol L^{-1} and 0.1

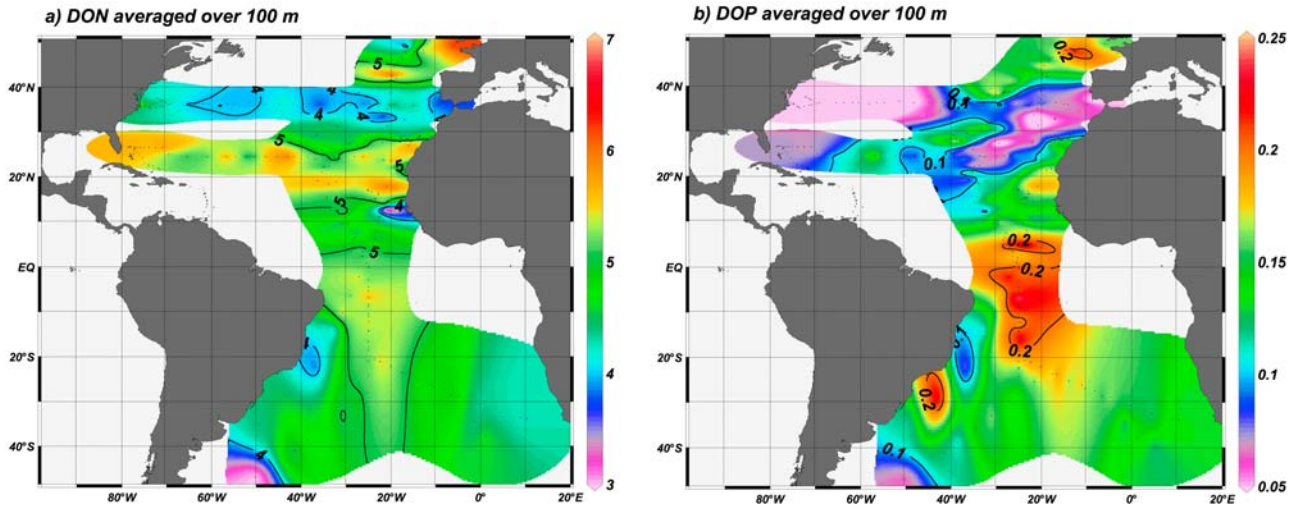

Figure 7. Composite maps of (a) DON and (b) DOP from data averaged over 100 m (μmol L^{-1}). Produced using Ocean Data View (Schlitzer, 2009).

to 0.2 μmol L^{-1}, respectively (Figures 6a and 6b). The standard deviations of DON and DOP (of the data making up the mean for each cell) are only slightly smaller than the mean, typically reaching 1 to 2 μmol L^{-1} and 0.1 to 0.2 μmol L^{-1}, respectively: the standard deviations are largest where the mean values are high, toward the eastern boundary in the North Atlantic subtropical gyre and around the tropics. Hence, there is significant variability in the DON and DOP for each region, as suggested in the meridional transects (Figures 3 and 4).

[24] Over most of the North Atlantic, there are typically 20 to 50 independent stations within each of these 10° cells (Figures 6c and 6d). Consequently, the standard errors for DON and DOP reduce to less than 1 μmol L^{-1} and 0.1 μmol L^{-1}, respectively (Figures 6c and 6d), which are always much less than the mean or standard deviations for each cell. Over the South Atlantic and parts of the western North Atlantic, the number of independent stations reduces to 10 or less, but the standard errors still appear to be relatively small, since the standard deviations are also small there. Thus, differences in the mean DON and DOP appear to be generally larger than the standard errors, suggesting the basin-scale patterns are reliable.

[25] Given this analysis, we now consider the basin-scale variations in DON and DOP formed from the average of the available data over the upper 100 m. The composite map for DON (Figure 7a) reveals maximum concentrations of 5 to 6 μmol L^{-1} at 18°N off North Africa, where there is intense upwelling, along 24.5°N in the western Atlantic and just south of the equator at 5°S, while there are local minima of 4 μmol L^{-1} along the northern flank of the subtropical gyre at 36°N and a narrow equatorial band along 5 to 10°N extending off North Africa (Figure 7a).

[26] The DOP distribution reveals a stronger contrast than seen in DON: there are generally elevated concentrations of 0.2 μmol L^{-1} in the South Atlantic subtropical gyre and depleted concentrations of less than 0.05 μmol L^{-1} over parts of the North Atlantic subtropical gyre (Figure 7b). Hence, DON and DOP appear to be cycled in a different manner in each basin, perhaps reflecting differences in the availability of nitrate and phosphate in each basin or differences in how bioavailable the DON and DOP are. Given these observed distributions, we next consider a model investigation.

4. Model Assessment of DON and DOP Transport and Its Effect on Export Production

[27] The role of DON and DOP in the Atlantic are now investigated using eddy-permitting experiments integrated for many decades, extending the previous coarse-resolution study of *Roussenov et al.* [2006].

4.1. Model Formulation and Physical Closures

[28] The model simulations have been conducted using an isopycnic model (MICOM 2.7) [*Bleck and Smith*, 1990] with a formulation similar to that employed by *Roussenov et al.* [2006], but with a higher horizontal resolution of 0.23° as in the work of *Roussenov et al.* [2008], rather than 1.4°. The physical and nutrient closures are briefly reviewed, although more details are provided by *Roussenov et al.* [2006].

[29] The model includes 15 σ_2 isopycnal layers in the vertical, plus a surface mixed layer with variable density. The model domain extends from 35°S to 65°N and from 98.5°W to 19°E with the topography taken from ETOP05 [*GEBCO*, 2003] data averaged within the model grid. At the northern and southern boundaries, sponge layers are incorporated below the mixed layer: isopycnal depths and salinity are relaxed toward climatology in relaxation zones extending for 8° in latitude on the southern boundary and 4° on the northern boundary with the relaxation time scale increasing from 30 days on the boundary to 180 days at the interior edge of the sponge layer. The Strait of Gibraltar is closed, but the salinity of subsurface layers close to the strait is relaxed to climatology on a 30 day relaxation time scale.

[30] Outside the mixed layer and these sponge layers, the only diapycnal mixing is achieved via a mixing coefficient, $\kappa = 10^{-7}$ m^2 s$^{-2}/N$, varying with buoyancy frequency N, which typically gives 4×10^{-5} m^2 s^{-1} for $N \sim 2.5 \times 10^{-3}$ s^{-1} within the main thermocline. In addition, the isopycnic model employs isopycnic mixing of tracers and thickness diffusion (using a diffusive velocity of 0.5 cm s^{-1} with Laplacian and biharmonic forms, respectively), and deformation-dependent momentum mixing (using a background mixing velocity of 1 cm s^{-1} with a Laplacian dependence).

[31] The dynamical model is initialized from Levitus climatology [*World Ocean Atlas*, 1998] and integrated for 60 years forced by NCEP monthly mean winds and surface fluxes in a repeating climatological mean year mode. Rivers are added as freshwater fluxes at corresponding coastal grid points. From year 60, the dynamical model is coupled with the nitrate/phosphate model with a setup similar to *Williams et al.* [2006] and *Roussenov et al.* [2006], and integrated for another 40 years [*Roussenov et al.*, 2008].

4.2. Nutrient Closures

[32] The physical model is coupled to a simplified nutrient model including inorganic and dissolved organic pools. Model integrations are conducted separately for nitrogen and phosphorus in order to reveal how differences in their recycling of organic matter affect export production.

[33] In each case, the total nutrient content is separated into a dissolved inorganic pool, dissolved organic matter (DOM) consisting of semilabile and refractory components, and particulate organic matter (POM). The organic matter in the model is only formed over the euphotic zone, which has a constant thickness of 100 m. The POM is assumed to fallout and be remineralized in the interior with a vertical remineralization scale of ~200 m [*Jenkins*, 1998; *Roussenov et al.*, 2006]. The dissolved inorganic, labile and refractory organic nutrients are transported by the circulation with life times in the euphotic zone of typically 6 months for the semilabile and 6–12 years for the refractory component, depending on the short wave radiation availability.

[34] The rate of consumption of the inorganic nutrients follows Michaelis-Menten kinetics with a dependence on the radiation intensity and the inorganic nutrient concentrations [see *Roussenov et al.*, 2006]. The consumed fraction of inorganic nutrients is split into POM and DOM related parts in a 50:50 ratio for nutrient rich waters (>5 μmol L^{-1} NO_3^-) and 35:65 in nutrient poor waters. The DOM is further split into semilabile and refractory fractions, which form the corresponding sources for the semilabile and refractory DOM.

[35] The initial nitrate is taken from climatology [*Conkright et al.*, 1994] while the semilabile DON and DOP are initialized to be 0 and the refractory DON initialized as 1 μmol L^{-1} (0.02 μmol L^{-1} for DOP). Along the southern closed boundary, nutrients are continuously relaxed to the initial condition within the buffer zones, and there are no atmospheric or riverine inputs of nutrients, nor any loss of nutrients on the seafloor through burial.

[36] The separate integrations for the nitrogen and phosphorus models use the same parameters in most of the model closures: maximum export rates, light dependence, similar split between DOM and particulate organic matter (POM), and decay time scales for the refractory and semilabile parts of DOM. The only important difference in the nitrogen and phosphorus recycling is related to the larger refractory component of DON; newly formed DON is assumed to be 50% semilabile and 50% refractory, while 95% of the newly formed DOP is assumed to be semilabile and only 5% refractory.

[37] The initial phosphate field is based on the initial nitrate field, assuming constant Redfield ratio N:P = 16:1. This type of initial state for the phosphate has been chosen, instead of climatological data, in order to allow the model to produce phosphate and DOP fields, depending entirely on the difference in the nitrogen and phosphate recycling in the nutrient model.

4.3. Modeled Nutrient Distributions

[38] The surface nutrient distributions and the effect of the organic nutrients in sustaining export production is now assessed; for more details of the background nutrient distributions, see *Roussenov et al.* [2006] and *Williams et al.* [2006].

4.3.1. Dissolved Inorganic Nutrients

[39] Meridional sections of nitrate and phosphate from the model reveal the expected surface oligotrophic waters over much of the subtropical and tropical Atlantic, overlying nutrient-rich waters within the underlying thermocline and associated nutricline (Figures 8a and 8b): the nutricline is raised toward the sea surface in the tropics and deepens over the subtropical gyres in the North and South Atlantic.

[40] Over the upper 100 m, the inorganic nutrients have elevated concentrations greater than 10 μmol L^{-1} for NO_3^- and 0.75 μmol L^{-1} for PO_4^{3-} at high latitudes over the subpolar gyre where convection and upwelling occur, as well as over the upwelling zones off the coast of Africa (Figures 9a and 9b). In contrast, there are relatively depleted nutrient concentrations, <0.4 μmol L^{-1} for NO_3^- and <0.05 μmol L^{-1} for PO_4^{3-}, over the subtropical gyres, where there is downwelling and limited convection.

[41] This snapshot reveals the advection of subtropical waters along the Gulf Stream carrying low concentrations of inorganic nutrients in the upper 100 m (Figures 9a and 9b). This signal is in contrast to the underlying, subsurface advection of nutrients with high concentrations along the Gulf Stream at depths of 200 m to 800 m [*Pelegrí and Csanady*, 1991; *Williams et al.*, 2006]. In addition, there are fine-scale filaments associated with the eddy transfer of nutrients over the basin, evident whenever there is sufficient gradient in the tracer.

[42] In comparison with the previous coarse-resolution study of *Roussenov et al.* [2006], this higher-resolution study leads to surface oligotrophic waters being more extensive over the North Atlantic subtropical gyre. The more vigorous horizontal circulation leads to an improved northward penetration of nutrient-rich waters in the nutrient stream linked with the Gulf Stream, which are transferred more realistically to higher latitudes, rather than midlatitudes.

4.3.2. Dissolved Organic Nutrients

[43] In the model, the dissolved organic nutrients are again concentrated within the surface waters, having the opposite relationship with the thermocline as seen for

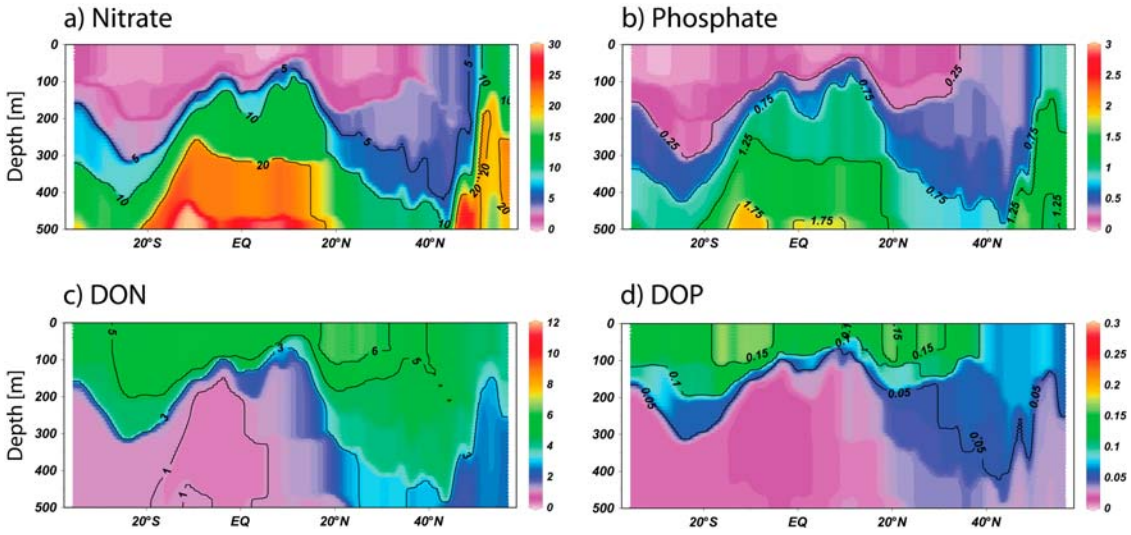

Figure 8. Modeled meridional sections along 25°W for (a) NO_3^-, (b) PO_4^{3-}, (c) DON, and (d) DOP (units for Figures 8a to 8d in μmol L^{-1}). Produced using Ocean Data View (Schlitzer, 2009).

inorganic nutrients (Figures 8c and 8d). The dissolved organic nutrients in the upper 100 m have their highest concentrations over the eastern side of the North Atlantic subtropical gyre and the central part of the South Atlantic subtropical gyre: concentrations of DON and DOP reach 5–6 μmol L^{-1} and 0.125–0.18 μmol L^{-1}, respectively (Figures 9c and 9d). The lowest concentrations of dissolved organic nutrients in the upper 100 m occur over the high latitudes (<4 μmol L^{-1} and <0.075 μmol L^{-1} for DON and DOP, respectively). At these latitudes the increase in convection leads to a dilution of the organic nutrients formed in the surface layer. Lowest concentrations occur also off the southwest coast of Africa at 20°S, where there is upwelling of deeper waters with low concentrations of DON and DOP [*Roussenov et al.*, 2006].

[44] While the observations of DON and DOP are noisier (Figures 3–7), there are broadly similar basin-scale patterns in the model: in both cases, high concentrations of DON occur along the equatorial flank and central parts of the subtropical gyres, and high concentrations of DOP occur in the South Atlantic subtropical gyre and off Africa at around 20°N. The observations differ from the model though in having slightly lower concentrations of DON along 36°N, as well as higher concentrations of DON and DOP in the northeast Atlantic around 45°N, which probably reflect shelf inputs (Figures 3–9). The model predicts lower concentrations of DON and DOP at higher latitudes in the subpolar gyre through the dilution effect of convection [*Roussenov et al.*, 2006].

[45] In comparison with the previous coarse-resolution model study, the eddy-permitting results have lower concentrations in DON and DOP over the North Atlantic subtropical gyre, reflecting how lower inorganic nutrient concentrations lead to less DON and DOP production. In the high-resolution case, the DON and DOP patterns have a finer-scale structure, revealing relatively elevated concentrations being transferred along the Gulf Stream and eddy transfer of high tracer concentrations from the African upwelling sites (Figures 9c and 9d).

[46] DON and DOP again provide important contributions to TDN and TDP, accounting for >80% of TDN and >60% of TDP over both the North Atlantic and South Atlantic subtropical gyres, and along the equator away from upwelling regions (Figures 9e and 9f). Low contributions (<50% of TDN and <30% of TDP) occur over subpolar regions due to dilution by winter deep convection, as well as over part of the upwelling zones off southwest and northwest Africa at 10°N and 25°S due to upwelled deep waters having low concentrations of DON and DOP (Figures 9e and 9f).

4.4. Modeled Effect of DON and DOP on Export Production

[47] The model estimates of particulate nitrogen (PN) and particulate phosphorus (PP) export reveal highest rates over subpolar areas and upwelling regions, reaching 0.3–0.4 mol N m^{-2} yr^{-1} and 20–30 mmol P m^{-2} yr^{-1}, while lower rates occur over much of the North Atlantic subtropical gyre, ~0.1 mol N m^{-2} yr^{-1} and 5–12 mmol P m^{-2} yr^{-1} for PN and PP, respectively (Figures 10a and 10b). Within the North Atlantic subtropical gyre, higher export rates occur along the eastern and equatorial sides, broadly following the plume of dissolved organic nutrients advected from the upwelling sites (Figures 9c and 9d). Whether these export estimates are realistic is difficult to assess: there is a slightly larger range in the inverse study of *Schlitzer* [2000], with a PN export rate of 0.4 mol N m^{-2} yr^{-1} in the tropics around 10°N and decreasing to less than 0.1 mol N m^{-2} yr^{-1} in the oligotrophic subtropical gyre at 40°N. Our model estimates are also slightly lower than in coarse model experiments [*Roussenov et al.*, 2006], as there are generally lower concentrations of surface inorganic nutrients in the tropics and subtropical gyres.

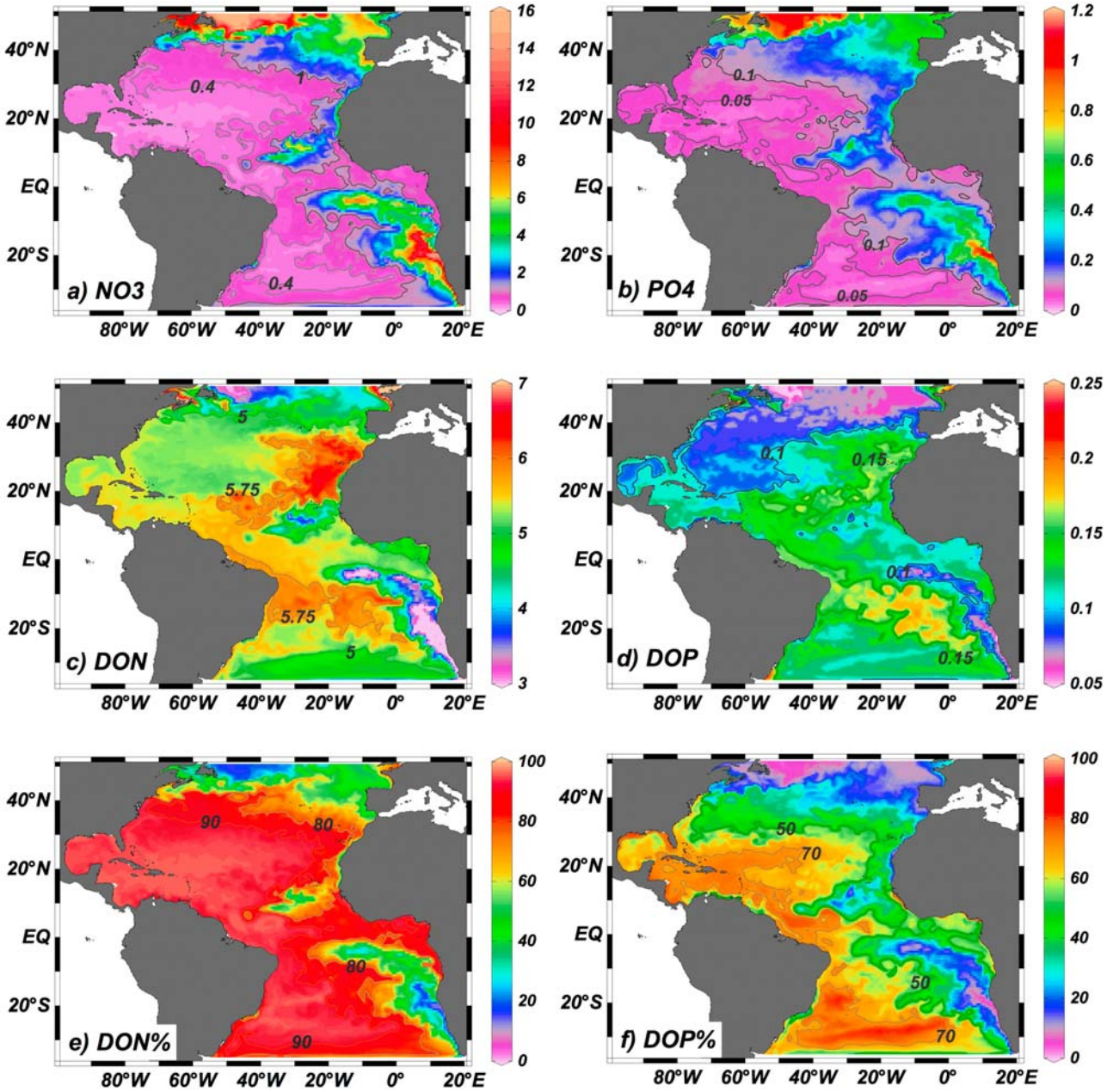

Figure 9. Modeled dissolved inorganic and organic nutrient distributions (μmol L^{-1}), and organic species fractions of total nutrients: (a) NO_3^-, (b) PO_4^{3-}, (c) DON, (d) DOP, (e) DON as a fraction of total nitrogen, and (f) DOP as a fraction of total phosphorus. All fields are for an average over the upper 100 m depth and for a snapshot for 1 January. Produced using Ocean Data View (Schlitzer, 2009).

[48] Accepting these caveats, the importance of DON and DOP inputs in sustaining export production is now assessed from the difference between two model integrations: the default integration including recycling of semilabile DOM and a separate integration where the DOM is assumed to be all refractory (so does not contribute to export production). These model evaluations are repeated separately for N and P.

[49] The model experiments reveal that semilabile DON inputs can sustain typically 40% or more of the PN export over the eastern and southern sides of the North Atlantic subtropical gyre (Figure 10c). The semilabile inputs of DOP are even more important in sustaining 60 to 70% of the PP export (Figure 10d). The role of DON and DOP in sustaining export production in these eddy-permitting integrations is surprisingly similar to that diagnosed in the coarse-resolution study [*Roussenov et al.*, 2006]. Thus, while the higher-resolution model has enabled a more vigorous circulation to develop with more plausible nutrient distributions, the effect of the semilabile inputs of DON and DOP on the export production is much the same. In both cases,

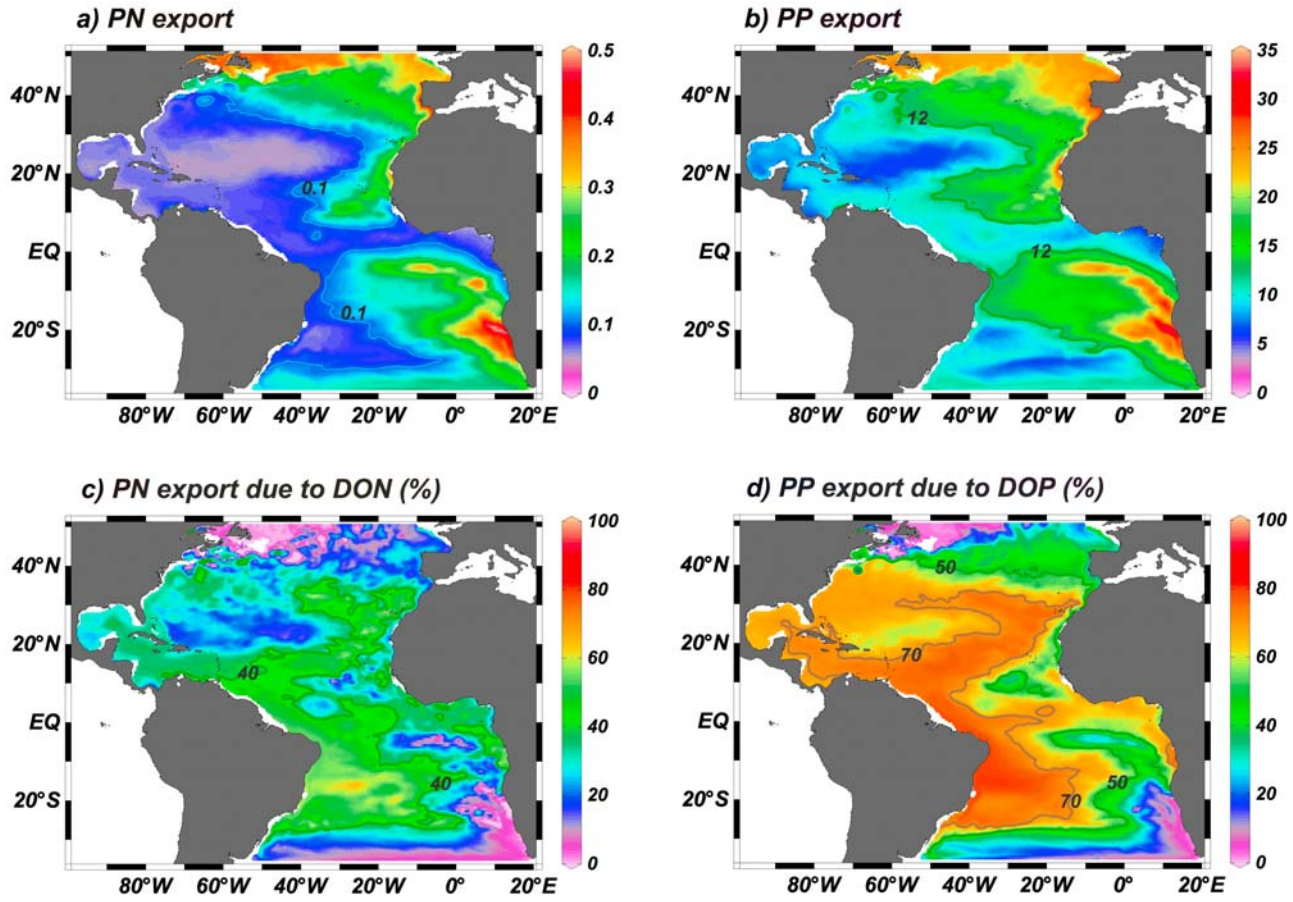

Figure 10. Modeled (a) particulate nitrogen, PN (mol m^{-2} yr^{-1}) and (b) phosphorus, PP (mmol m^{-2} yr^{-1}) export production, and fraction of PN and PP export due to (c) DON and (d) DOP. Produced using Ocean Data View (Schlitzer, 2009).

the DON and DOP inputs play a central role over the eastern side of the subtropical gyres.

[50] While the end result is much the same, the mechanism by which the DON and DOP is transferred from their sources at the eastern boundary and tropics into the gyre interior does vary: in the higher-resolution case, eddy lateral transfer of the tracers occurs, while in the coarser model the background gyre circulation and isopycnic diffusion provides the transfer.

5. Discussion

[51] The role of DON and DOP are assessed here through a combined observational and modeling study. Distributions of DON and DOP are diagnosed through 8 recent transects over the Atlantic Ocean. The DON and DOP concentrations are surface intensified with greater values above the thermocline, where they provide the dominant contributions to the total dissolved nitrogen and phosphorus pools. There are elevated concentrations of DON over the upper 100 m close to the African upwelling zone at 18°N and south of the equator around 10°S, as well as lower values at 36°N. There are stronger basin-scale contrasts in DOP, generally higher values also over the African upwelling zone and the South Atlantic subtropical gyre, but very low concentrations over much of the North Atlantic subtropical gyre.

[52] The reduced DOP in the North Atlantic subtropical gyre coincides with very low surface phosphate concentrations and probably reflects increased utilization of DOP [*Mather et al.*, 2008]. Enhanced cycling and utilization of DOP is indeed expected north of the equator in the tropical Atlantic, where there is enhanced nitrogen fixation [*Dyhrman et al.*, 2006; *Sohm and Capone*, 2006; *Reynolds et al.*, 2007], probably sustained by iron supplied via Saharan dust inputs [*Mills et al.*, 2004; *Jickells et al.*, 2005].

[53] While there is variability in the distribution of organic nutrients, the large-scale patterns shown are consistent with the hypothesis put forward; these organic nutrients are produced at the eastern margin of the North Atlantic subtropical gyre and over the equatorial region, and are then redistributed toward the gyre interior, therefore providing an additional source of nutrients to sustain carbon export.

[54] In support of this view, the accompanying model study shows that the DON and DOP are generated along the eastern boundary of the North Atlantic subtropical gyre and

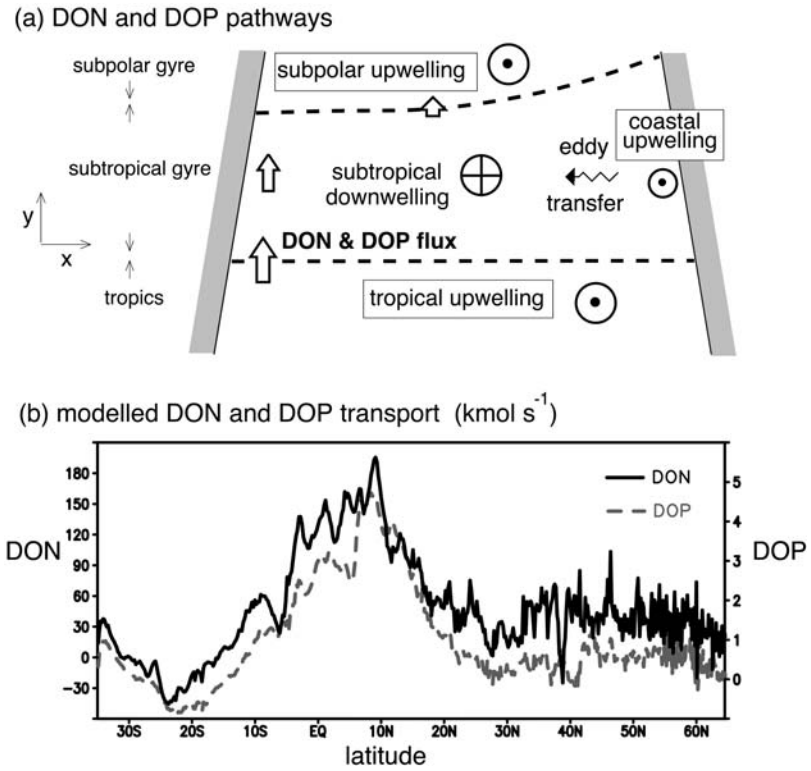

Figure 11. (a) Schematic figure depicting the formation and transport of dissolved organic nutrients; (b) Model diagnostics of the northward transport (kmol s^{-1}) of DON (full line) and DOP (dashed line) averaged over the upper 600 m and across the width of the basin: there is a northward transport from the tropics, which is greater for DON due to its higher refractory content than for DOP.

the tropics through the consumption of inorganic nutrients (Figure 11a), sustained by the vertical upwelling of nutrient-rich thermocline and deep waters. The DON and DOP are then transferred into the interior of the North Atlantic subtropical gyre through a lateral transfer, achieved partly by mesoscale eddies; this pathway is more clearly revealed in this eddy-permitting study than in the previous coarse-model assessment of *Roussenov et al.* [2006], where there were smoother distributions of DON and DOP. The DON and DOP are systematically transported northward over the basin as part of the overturning circulation, where the northward flux of DON and DOP is greatest at 10°N reaching 180 kmol s^{-1} and 4 kmol s^{-1} over the upper 600 m, respectively, and then progressively decreases northward (Figure 11b); the flux of DOP is smaller than that of DON due to the DOP being more labile and so having very low concentrations at depth.

[55] The model study suggests that transport and cycling of DON and DOP does help to support export production over the oligotrophic gyres: inputs of semilabile DON sustain typically 40% of the PN export over the subtropical gyres, while inputs of semilabile DOP support typically 70% of PP export over the eastern and southern flanks of the North Atlantic subtropical gyre. Hence, the cycling of DOP appears to be more important than that of DON for the North Atlantic, probably reflecting both how more of the DOP is semilabile than in the DON pool and how it is more difficult to supply phosphorus to surface waters than nitrogen in the North Atlantic.

[56] In summary, DON and DOP play a central role in the nutrient cycling of the oligotrophic Atlantic, dominating the total nutrient pools in the surface waters, and helping to sustain the export production on the eastern and central sides of the basin, but are less important on the western sides of the basin. Given this important role, it is likely that DON and DOP have a similar effect in surface waters of other oligotrophic systems, including other subtropical gyres, the Mediterranean Sea and summer, stratified shelf seas.

[57] **Acknowledgments.** This study was supported by the U.K. Natural Environment Research Council through the 36°N consortium (NER/O/S/2003/00625) and Atlantic Meridional Transect consortium (NER/O/S/2001/00680). We are grateful for the following assistance: Malcolm Woodward and Katie Chamberlain (Plymouth Marine Laboratory) measured inorganic nutrients onboard AMT cruises; Neil Jenkinson provided support with UV systems; and Sarah Root, Mark Stinchcome, and Tim Adey assisted with the collection of samples for total nutrient analysis. We are very grateful to two anonymous reviewers for their constructive comments. Most figures were produced using Ocean Data View (R. Schlitzer, Ocean data view, 2009, available at http://odv.awi.de).

References

Abell, J., S. Emerson, and P. Renaud (2000), Distributions of TOP, TON and TOC in the North Pacific subtropical gyre: Implications for nutrient

supply in the surface ocean and remineralization in the upper thermocline, *J. Mar. Res.*, *58*(2), 203–222.
Alvarez-Salgado, X. A., and A. E. J. Miller (1998), Simultaneous determination of dissolved organic carbon and total dissolved nitrogen in seawater by high temperature catalytic oxidation: Conditions for precise shipboard measurements, *Mar. Chem.*, *62*, 325–333.
Antia, N. J., P. J. Harrison, and L. Oliveira (1991), The role of dissolved organic nitrogen in phytoplankton nutrition, cell biology and ecology, *Phycologia*, *30*(1), 1–89.
Baker, A. R., S. D. Kelly, K. F. Biswas, M. Witt, and T. D. Jickells (2003), Atmospheric deposition of nutrients to the Atlantic Ocean, *Geophys. Res. Lett.*, *30*(24), 2296, doi:10.1029/2003GL018518.
Bale, T. (2005), Atlantic Meridional Transect. AMT16 Cruise Report. RRS *Discovery*. 20 May–June 2005, technical report, Plymouth Mar. Lab., Plymouth, U. K.
Berman, T., and D. A. Bronk (2003), Dissolved organic nitrogen: A dynamic participant in aquatic ecosystems, *Aquat. Microbial Ecol.*, *31*(3), 279–305.
Björkman, K., A. L. Thomson-Bulldis, and D. M. Karl (2000), Phosphorus dynamics in the North Pacific subtropical gyre, *Aquat. Microbial Ecol.*, *22*, 185–198.
Bleck, R., and L. T. Smith (1990), A wind-driven isopycnic coordinate model of the North and equatorial Atlantic Ocean: 1. Model development and supporting experiments, *J. Geophys. Res.*, *95*, 2373–3285.
Bronk, D. A. (2002), Dynamics of DON, in *Biogeochemistry of Marine Dissolved Organic Matter*, edited by D. A. Hansell and C. A. Carlson, pp. 153–247, Acad. Press, New York.
Bronk, D. A., M. W. Lomas, P. M. Glibert, K. J. Schukert, and M. P. Sanderson (2000), Total dissolved nitrogen analysis: Comparisons between persulfate, UV and high temperature oxidation methods, *Mar. Chem.*, *69*, 163–178.
Bronk, D. A., J. H. See, P. Bradley, and L. Killberg (2007), DON as a source of bioavailable nitrogen for phytoplankton, *Biogeosciences*, *4*, 283–296.
Bryden, H. L., H. R. Longworth, and S. A. Cunningham (2005), Slowing of the Atlantic meridional overturning circulation at 25°N, *Nature*, *438*, 655–657, doi:10.1038/nature04385.
Bushaw, K. L., R. G. Zepp, M. A. Tarr, D. Schular-Jander, R. A. Bourboniere, R. E. Hodson, W. L. Miller, D. A. Bronk, and M. A. Moran (1996), Photochemical release of biologicaly available nitrogen from aquatic dissolved organic matter, *Nature*, *381*, 404–407.
Clark, L. L., E. D. Ingall, and R. Benner (1998), Marine phosphorus is selectively remineralized, *Nature*, *393*, 881, doi:10.1038/30.
Conkright, M. E., S. Levitus, and T. P. Boyer (1994), *World Ocean Atlas 1994*s, vol. 1, *Nutrients*, *NOAA Atlas NESDIS 1*, 155 pp., NOAA, Silver Spring, Md.
Cunningham, S. A. (2005), RRS *Discovery* Cruise D279. 04 April–10 May 2004. A Trans-Atlantic Hydrographic Section at 24.5°N, Cruise Report 54, technical report, Natl. Oceanogr. Cent., Southampton, U. K.
Dyhrman, S. T., P. D. Chappell, S. T. Haley, J. W. Moffet, E. D. Orchard, J. B. Waterbury, and E. A. Webb (2006), Phosphate utilization by the globally important marine diazotroph *trichodesmium*, *Nature*, *439*, 68–71, doi:10.1038/nature04203.
Emerson, S., P. Quay, D. Karl, C. Winn, L. Tupas, and M. Landry (1997), Experimental determination of the organic carbon flux from open-ocean surface waters, *Nature*, *389*(6654), 951–954.
Emerson, S., S. Mecking, and J. Abell (2001), The biological pump in the subtropical North Pacific Ocean: Nutrient sources, Redfield ratios, and recent changes, *Global Biogeochem. Cycles*, *15*(3), 535–554.
Gallienne, C. (2000), Atlantic Meridional Transect. Cruise Report AMT10. 12th April–8th May 2000. Montevideo (Uruguay) to Grimsby (UK), technical report, Plymouth Mar. Lab., Plymouth, U. K.
GEBCO (2003), *The Centenary Edition of the GEBCO Digital Atlas [CDROM]*, BODC, Liverpool, U. K., April.
Holligan, P. (2004), RRS *James Clark Ross*. 28 April–1 June 2004, AMT 14 Cruise Report, technical report, National Oceanogr. Cent., Southampton, U. K.
Holligan, P. (2005), Atlantic Meridional Transect. AMT17 cruise report. RRS *Discovery*, 15 October–28 November 2005, technical report, Natl. Oceanogr. Cent., Southampton, U. K.
Jenkins, W. J. (1982), Oxygen utilization rates in the North Atlantic subtropical gyre and primary production in oligotrophic systems, *Nature*, *300*(5889), 246–248.
Jenkins, W. J. (1998), Studying subtropical thermocline ventilation and circulation using tritium and ^{3}He, *J. Geophys. Res.*, *103*(C8), 15,817–15,831.
Jenkins, W. J., and J. C. Goldman (1985), Seasonal oxygen cycling and primary production in the Sargasso Sea, *J. Mar. Res.*, *43*, 465–491.
Jickells, T. (2003), RRS *James Clark Ross Cruise* 90. 12 May–17 June 2003, AMT12, *UEA Cruise Rep. Ser. 8*, Univ. of East Anglia, Norwich, U. K.
Jickells, T. D., et al. (2005), Global iron connections between desert dust, ocean biogeochemistry, and climate, *Science*, *308*, 67–71, doi:10.1126/science.1105959.
Karl, D. M., and K. M. Björkman (2002), Dynamics of DOP, in *Biogeochemistry of Marine Dissolved Organic Matter*, edited by D. A. Hansell and C. A. Carlson, pp. 249–366, Acad. Press, New York.
Karl, D. M., and K. Yanagi (1997), Partial characterization of the dissolved organic phosphorus pool in the oligotrophic North Pacific Ocean, *Limnol. Oceanogr.*, *42*(6), 1398–1405.
Kolowith, L. C., E. D. Ingall, and R. Benner (2001), Composition and cycling of marine organic phosphorus, *Limnol. Oceanogr.*, *46*(2), 309–320.
Landolfi, A. (2005), The importance of dissolved organic nutrients in the biogeochemistry of oligotrophic gyres, Ph.D. thesis, School of Ocean and Earth Sci., Univ. of Southampton, Southampton, U. K.
Landolfi, A., A. Oschlies, and R. Sanders (2008), Organic nutrients and excess nitrogen in the North Atlantic subtropical gyre, *Biogeosciences*, *5*, 1199–1213.
Mahaffey, C., R. G. Williams, G. A. Wolff, and W. T. Anderson (2004), Physical supply of nitrogen to phytoplankton in the Atlantic Ocean, *Global Biogeochem. Cycles*, *18*, GB1034, doi:10.1029/2003GB002129.
Mather, R. L., S. E. Reynolds, G. A. Wolff, R. G. Williams, S. Torres-Valdes, X. Pan, E. M. S. Woodward, R. Sanders, and E. P. Achterberg (2008), Phosphorus cycling in the North and South Atlantic Ocean subtropical gyres, *Nat. Geosci.*, *1*, 439–443, doi:10.1038/ngeo232.
McDonagh, E. L. (2007), RSS Charles Darwin Cruise CD171. 1 May–15 June 2005. A Trans-Atlantic Hydrographic Section at 36°N, Cruise Report 14, techincal report, Natl. Oceanogr. Cent., Southampton, U. K.
McGillicuddy, D. J., A. R. Robinson, D. A. Siegel, H. W. Jannasch, R. Johnsonk, T. D. Dickey, J. McNeil, A. F. Michaels, and A. H. Knapk (1998), Influence of mesoscale eddies on new production in the Sargasso Sea, *Nature*, *394*, 263–266.
Mills, M. M., C. Ridame, M. Davey, J. La Roche, and R. J. Geider (2004), Iron and phosphorus co-limit nitrogen fixation in the eastern tropical North Atlantic, *Nature*, *429*, 292–294.
Moutin, T., D. M. Karl, S. Duhamel, P. Rimmelin, P. Raimbault, B. A. S. Vaan Mooy, and H. Claustre (2008), Phosphate availability and the ultimate control of new nitrogen input by nitrogen fixation in the tropical Pacific Ocean, *Biogeosciences*, *5*, 95–109.
Pelegrí, J. L., and G. T. Csanady (1991), Nutrient trnsport and mixing in the Gulf Stream, *J. Geophys. Res.*, *96*, 2577–2583.
Pelegrí, J. L., A. Marrero-Díaz, and A. W. Ratsimandresy (2006), Nutrient irrigation of the North Atlantic, *Progr. Oceanogr.*, *70*, 366–406.
Rees, A. (2004), RRS *Discovery* Cruise 284. 17 September–29 October 2004, Atlantic AMT15 Cruise Report, technical report, Plymouth Mar. Lab., Plymouth, U. K.
Reynolds, S. E., R. L. Mather, G. A. Wolff, R. G. Williams, A. Landolfi, R. Sanders, and E. M. S. Woodward (2007), How widespread and important is N_2 fixation in the North Atlantic Ocean?, *Global Biogeochem. Cycles*, *21*, GB4015, doi:10.1029/2006GB002886.
Robinson, C., P. Holligan, and T. Jickells (2006a), The Atlantic Meridional Transect Programme, *Deep Sea Res., Part II*, *53*(14–16), 1483–1484, doi:10.1016/j.dsr2.2006.06.002.
Robinson, C., et al. (2006b), The Atlantic Meridional Transect (AMT) Programme: A contextual view 1995–2005, *Deep Sea Res., Part II*, *53*(14–16), 1485–1515, doi:10.1016/j.dsr2.2006.05.015.
Roussenov, V., R. G. Williams, C. Mahaffey, and G. A. Wolff (2006), Does the transport of dissolved organic nutrients affect export production in the Atlantic Ocean?, *Global Biogeochem. Cycles*, *20*, GB3002, doi:10.1029/2005GB002510.
Roussenov, V. M., R. G. Williams, C. W. Hughes, and R. J. Bingham (2008), Boundary wave communication of bottom pressure and overturning changes for the North Atlantic, *J. Geophys. Res.*, *113*, C08042, doi:10.1029/2007JC004501.
Sanders, R., and T. Jickells (2000), Total organic nutrients in Drake Passage, *Deep Sea Res., I*, *47*, 997–1014.
Sanders, R., L. Brown, S. Henson, and M. Lucas (2005), New production in the Irminger Basin during 2002, *J. Mar. Syst.*, *55*, 291–310.
Schlitzer, R. (2000), *Inverse Methods in Biogeochemical Cycles*, *Geophys. Monogr. Ser.*, vol. 114, pp. 107–124, AGU, Washington, D. C.
Sharp, J. H. (2002), Analytical methods for total DOM pools, in *Biogeochemistry of Marine Dissolved Organic Matter*, edited by D. A. Hansell and C. A. Carlson, pp. 35–58, Acad. Press, New York.

Sohm, J. A., and D. G. Capone (2006), Phosphorus dynamics of the tropical and subtropical North Atlantic: *Trichodesmium* spp. versus bulk plankton, *Mar. Ecol. Prog. Ser.*, *317*, 21–28.

Valderrama, J. C. (1981), The simultaneous analysis of total nitrogen and total phosphorus in natural waters, *Mar. Chem.*, *10*(2), 109–122.

Vidal, M., C. M. Duarte, and S. Agusti (1999), Dissolved organic nitrogen and phosphorus pools and fluxes in the central Atlantic Ocean, *Limnol. Oceanogr.*, *44*(1), 106–115.

Williams, R. G., and M. J. Follows (1998), The Ekman transfer of nutrients and maintenance of new production over the North Atlantic, *Deep Sea Res., Part I*, *45*(2–3), 461–489.

Williams, R. G., and M. J. Follows (2003), Physical transport of nutrients and the maintenance of biological production, in *Ocean Biogeochemistry: The Role of the Ocean Carbon Cycle in Global Change*, edited by M. Fasham, pp. 19–51, Springer, New York.

Williams, R. G., V. Roussenov, and M. J. Follows (2006), Nutrient streams and their induction into the mixed layer, *Global Biogeochem. Cycles*, *20*, GB1016, doi:10.1029/2005GB002586.

World Ocean Atlas (1998), *NODC (Levitus) World Ocean Atlas 1998*, data provided by the NOAA-CIRES Clim, Diagn. Cent., Boulder, Colo. (Available at http://www.cdc.noaa.gov)

E. P. Achterberg, R. Sanders, and S. Torres-Valdés, Ocean Biogeochemistry and Ecosystems Research Group, National Oceanography Centre, University of Southampton, European Way, Southampton, SO14 3ZH, UK. (sinhue@noc.soton.ac.uk)

A. Landolfi, Marine Biogeochemie, Leibniz-Institut Für Meereswissenschaften, Düsternbrooker Weg 20, D-24105, Kiel, Germany.

R. Mather, V. M. Roussenov, R. G. Williams, and G. A. Wolff, Department of Earth and Ocean Sciences, University of Liverpool, Liverpool, L69 3BX, UK.

X. Pan and S. Reynolds, British Oceanographic Data Centre, 6 Brownlow St., Liverpool, L3 5DA, UK.